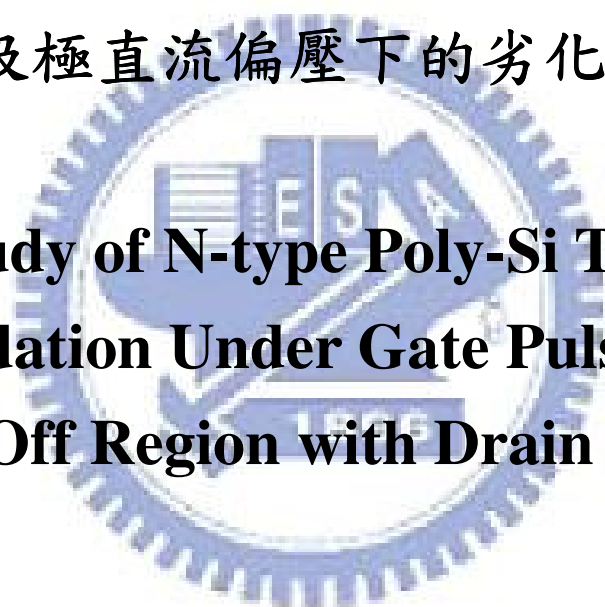


國立交通大學

顯示科技研究所

碩士論文

N 型複晶矽薄膜電晶體在閘極負電壓脈
波汲極直流偏壓下的劣化研究



**Study of N-type Poly-Si TFTs
Degradation Under Gate Pulse Stress
in Off Region with Drain Bias**

研究生:施偉倫

Wei-Lun Shih

指導教授:戴亞翔 博士

Dr. Ya-Hsiang Tai

中華民國 九十六 年 六 月

**N 型複晶矽薄膜電晶體在閘極負電壓脈
波汲極直流偏壓下的劣化研究**

**Study of N-type Poly-Si TFTs Degradation
Under Gate Pulse Stress in Off Region
with Drain Bias**

研 究 生：施偉倫

Student : Wei-Lun Shih

指 導 教 授：戴亞翔 博士

Advisor : Dr. Ya-Hsiang Tai



A Thesis

Submitted to Department of Photonics
Institute of Display

College of Electrical Engineering and Computer Science

National Chiao Tung University

in Partial Fulfillment of the Requirements

for the Degree of

Master

in

Display

June 2007

Hsinchu, Taiwan, Republic of China

中 華 民 國 九 十 六 年 六 月

N 型複晶矽薄膜電晶體在閘極負電壓脈波 汲極直流偏壓下的劣化研究

研究生：施偉倫

指導教授：戴亞翔 博士

國立交通大學

顯示科技研究所

摘要

複晶矽薄膜電晶體(poly-Si TFT)因為其優異的元件特性，最近幾年在液晶顯示器(AMLCD)及有機發光二極體(AMOLED)顯示器應用中之所以會是眾所注目的焦點。相較非晶矽薄膜電晶體，複晶矽薄膜電晶體有較高電流趨動能力及較好的可靠度，因此在複晶矽薄膜電晶體顯示器裡，它可以被用來整合畫素電路及周邊驅動電路於同一片玻璃基板上，如此使面板結構簡單化且可以減少週邊半導體零組件的使用數量以及後段模組在組裝時的接點數目，進而提高工程可靠度，除此之外更可降低驅動 IC 成本，維持低耗電特性，提供高精細的畫質表現。所以，複晶矽薄膜電晶體被視為實現系統化面板(System on Panel)的關鍵技術。

然而不同於畫素的薄膜電晶體，在驅動電路上的薄膜電晶體會受到高頻的閘極脈波電壓所驅動。因此，薄膜晶體在交流訊號操作下的劣化機制必須要仔細的探討。

在這篇論文中，我們研究了低溫複晶矽薄膜電晶體在閘極負偏壓脈波且汲極直流偏壓的劣化，我們觀察到在汲極端會有一個嚴重的劣化，當閘極操作在負偏壓交流訊號且汲極直流偏壓下會量測到一個電流(在此我們稱為 pump

current)。汲極和源極有不同的電場效應，因此，在此電流經過時，也在這兩端產生不一樣的劣化行為。我們也觀察到元件的劣化和汲極端的電壓、閘極電壓上升時間、閘極電壓下降時間、閘極電壓的範圍很有關係。我們可以用量到的 pump current 來解釋不同操作情況下對元件的劣化行為。這個發現幫助我們在研究 LTPS 元件的可靠度上，了解並估計元件的劣化機制並在設計元件上面提供了一個參考。



Study of N-type Poly-Si TFTs Degradation Under Gate Pulse Stress in Off Region with Drain Bias

Student: Wei-Lun Shih

Advisor: Dr. Ya-Hsiang Tai

**Department of Display Institute,
National Chiao Tung University**

Abstract

Polycrystalline silicon (poly-Si) thin film transistors (TFTs) have recently attracted much attention in the application on the integrated peripheral circuits of active matrix liquid crystal displays (AMLCDs) and active matrix organic light emitting diode (AMOLED) displays. The significant advantages over amorphous silicon (a-Si) TFTs are in the higher current driving capability and the better reliability. In poly-Si TFT-controlled displays, poly-Si TFTs are used to implement pixel circuits and driving circuits on a single glass substrate to reduce system cost and possess compact module. Therefore, the poly-Si TFT is the best candidate to realize system-on-panel (SOP).

However, unlike pixel TFTs, TFTs in driver circuits are subjected to high-frequency voltage pulses. Therefore, the degradation mechanism under dynamic operation should be understood in detail.

In this thesis, the device degradation of low-temperature polycrystalline thin film transistor under gate AC stress in off region with drain bias has been investigated. The effective drain current, pumped by the AC gate voltages in the off region, undergoes different electric field effects near the source and drain junction and therefore results

in different degradation behavior near these two regions. It is noticed that the degradation depends profoundly on the DC drain bias. It is also affected by the rising time T_r , falling time T_f , and the V_g range. This finding would be helpful in the understanding and evaluation of the device degradation mechanism and provide a guideline to design for reliability of poly-Si TFT circuit.



致謝

感謝我的指導教授 戴亞翔博士，老師不僅僅對於學術研究上的指導，還有對於人生規劃及待人處世上的態度上都使我獲益良多，尤其是趕論文的這段期間，感謝老師的在百忙之中批改以及教導，在這求學的過程中，都對我有啟發性的影響。

感謝學長姐們，士哲、彥甫、泓緯、皓彥、一德、士欽、浩麟、國烽、鈺函、可青、建焜、婉萍、俊文、娟姐，謝謝你們不厭其煩的解決我許多課業上的問題，適時的督促我讓我往前邁進。

感謝實驗室的同學以及學弟妹們，育德、晉煒、振業、亞諭、建名、秀娟、曉嫻、長龍、明憲、小黑、首席、翔帥、阿貴、立煒，不管是在課業上或是生活上，你們總會適時的伸出援手，和你們的相處是我兩年來最快樂的時光，一起走過一起奮鬥的足跡我永遠也不會忘記。

感謝我的好朋友們，感謝你們長久以來的扶持與關懷，在我需要幫助的時候你們從來都不曾缺席。

最後我要感謝，我最親愛的家人們，如果我有一點點的貢獻與成長，都是來自你們真誠無私的愛與無可替代的存在。

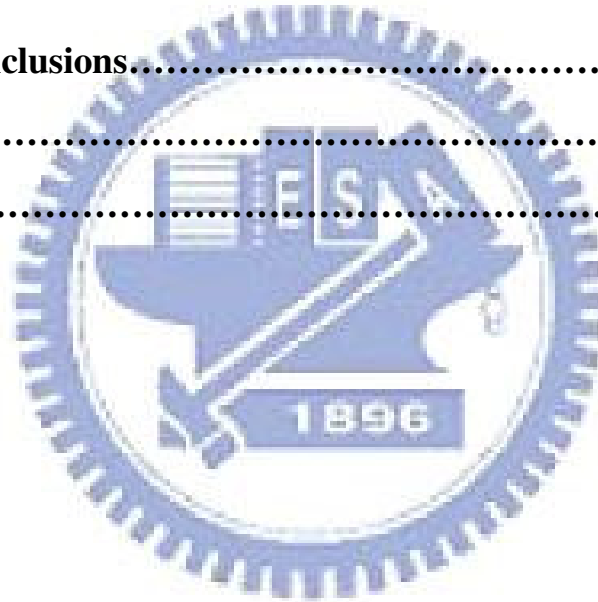
「撰寫論文的過程大多是孤獨而寂寞的，但是有了諸位的幫助與點滴的幫助，卻使我的心如五月的陽光般和煦。」最後感謝所有曾經幫助過我的朋友們，謝謝你們一路上給我的支持與關心，我今天才可以完成碩士學位。

偉倫 2007.06.25

Contents

Chinese Abstract	III
English Abstract	V
Acknowledgement	VII
Contents	VIII
Figure Captions	X
Chapter 1 Introduction	1
1.1 Overview of Low-Temperature Polycrystalline Silicon Thin Film Transistors (LTPS TFTs).....	1
1.2 Review of Studies on TFT under DC and AC Stress.....	3
1.2.1 DC stress.....	3
1.2.2 AC stress.....	5
1.3 Motivation.....	12
1.4 Thesis Organization.....	14
Chapter 2 Experiments	16
2.1 Procedures of Fabrication of LTPS TFTs.....	16
2.2 AC Stress Conditions.....	17
2.3 Extraction of Device Electrical Parameters.....	21
Chapter 3 AC Stress with Drain Bias Effect	24
3.1 Degradation of I-V Behavior.....	24
3.1.1 Effect of drain bias.....	24
3.1.2 Damage region.....	26
3.2 Degradation of C-V Behaviors.....	29
3.2.1 Slicing circuit model.....	29

3.2.2 Gate-source capacitance and gate-drain capacitance	31
3.3 Electric Field Simulation.....	35
3.4 Off Region AC Stress with Drain and Source Bias.....	39
3.5 Degradation Model and Pump Current.....	43
Chapter 4 Other Effect.....	48
4.1 Duty Ratio.....	48
4.2 Rising Time.....	50
4.3 Falling Time.....	55
4.4 V_g Range Effect.....	60
Chapter 5 Conclusions.....	69
References.....	70
Vita.....	73



Figures Captions

Chapter 1

Figure 1-1 Stress voltage dependence of the V_T shift of the TFTs

Figure 1-2 Dependence of stress voltage on the I_{on} variation in the TFTs

Figure 1-3 A schematic diagram for degradation model of the poly-Si TFT.

Figure 1-4 Dependence on the number of pulse repetitions of n-channel TFT

Figure 1-5(a) Swing region

Figure 1-5(b) Dependence of degradation on swing region for n-channel TFT

Figure 1-6(a) Rising time dependence of the degradation

Figure 1-6(b) Falling time dependence of the degradation

Figure 1-7(a) Degradation of μ/μ_0 in n-channel TFT under AC stress with $V_g = -15$ V to 0 V measured for various rising times T_r and for $T_f = 100$ ns

Figure 1-7(b) Degradation of μ/μ_0 in n-channel TFT under AC stress with $V_g = -15$ V to 0 V measured for various rising times T_f and for $T_r = 100$ ns

Figure 1-8 Previous researches of LTPS TFT reliability

Figure 1-9 Three Level Gate Drive (gate off region AC stress with drain bias)

Chapter 2

Figure 2-1 The cross-section views of n-channel LTPS TFTs with LDD structure

Figure 2-2 Waveform and definition of the AC signal

Table 2-1 four stress conditions summary (Frequency=500k Hz, stress 60s)

Figure 2-3 TFT under AC stress with various drain bias while source is grounded

Figure 2-4 TFT under gate AC stress with various rising time with drain bias 20V

Figure 2-5 TFT under gate AC stress with various falling time with drain bias 20V

Figure 2-6 TFT under various V_g range stress with drain bias

Chapter 3

Figure 3-1(a) Id-Vg curves before and after dynamic gate stress (Frequency=500 kHz, stress 60 s) with different drain bias voltages

Figure 3-1(b) Dependence of the mobility on V_{DS} with gate AC stress in off region

Figure 3-1(c) Dependence of the S.S on V_{DS} with gate AC stress in off region

Figure 3-2 (a) Forward saturation current (measure $V_{DS} = 10V$)

Figure 3-2 (b) Reverse saturation current (measure $V_{DS} = 10V$)

Figure 3-3(a). The n-type device cross section

Figure 3-3(b)The n-type slicing circuits.

Figure 3-4(a) The slicing circuit that the R_{ch} is short when gate voltage is much higher than the V_{th} .

Figure 3-4(b) The slicing circuit that the R_{ch} is open when gate voltage is far below the V_{th} .

Figure 3-5 (a) C_{GS} measurement configuration.

Figure 3-5 (b) Normalized C_{GS} curves versus gate voltage after AC stress with drain bias measured at frequency of 1M Hz.

Figure 3-6 (a) C_{GD} measurement configuration.

Figure 3-6 (b) Normalized C_{GD} curves versus gate voltage after AC stress with drain bias measured at frequency of 1M Hz.

Figure 3-7 The modified slicing circuit with large resistance R_{ch}' near drain region after stress.

Figure 3-8 The electric field distribution for gate voltage of -15V and source/drain grounded ($V_S=0V, V_g=-15V, V_D=0V$)

Figure 3-9 The electric field distribution for gate voltage of -15V, source grounded, and drain bias of 20V ($V_S=0V, V_g=-15V, V_D=20V$)

Figure 3-10 The electric field absolute value under gate voltage of -15V and source grounded with various drain bias

Figure 3-11 The maximal electric field under gate voltage of -15V and source grounded with various drain bias

Figure 3-12 The vertical electric field distribution along the channel.

Figure 3-13 The lateral electric field distribution along the channel.

Figure 3-14 TFT under gate AC stress in off region with drain and source 20V

Figure 3-15 Electric field distribution when $V_S=20V$ $V_G=-15V$, and $V_D=20V$.

Figure 3-16 The electric field absolute value under gate AC stress with various source and drain bias

Figure 3-17 I_D-V_G and mobility extract under various stress condition

Figure 3-18 Normalized C_{GS} curves under gate AC stress with various source and drain bias measured at frequency of 1M Hz.

Figure 3-19 Normalized C_{GD} curves under gate AC stress with various source and drain bias measured at frequency of 1M Hz.

Figure 3-20 The proposed AC stress degradation model in TFT structure with source and drain grounded when V_g swings (a) from 0V to -15V and (b) from -15V to 0V.

Figure 3-21(a) The proposed AC stress degradation model in TFT structure with drain bias voltage when V_g swings from 0V to -15V

Figure 3-21(b) The proposed AC stress degradation model in TFT structure with drain bias voltage when V_g swings from -15V to 0V.

Figure 3-21(c) The proposed AC stress degradation model in TFT structure with drain bias voltage

Figure 3-22 The measured DC drain currents under AC gate stress in the off region with various drain voltages.

Chapter 4

Table 4-1 Four stress conditions summary (Frequency=500 kHz, Stress time=60s)

Figure 4-1 The pumped current measure under various gate pulse duty ratio

Figure 4-2 The measured DC drain currents under various gate pulse duty ratio

Table 4-2 Setting of time for the experiment of T_r from 100ns to 700ns

(Frequency=500 kHz, Stress time 60s)

Figure 4-3 The three stressed condition with T_r from 100ns to 700ns

Figure 4-4(a) Dependence of the mobility after gate AC stress in the off region on rising time

Figure 4-4(b) Dependence of the S.S. after gate AC stress in the off region on rising time

Figure 4-5 The pump current under various gate pulse rising time

Figure 4-6 The measured DC drain current versus stress time under gate pulses with various rising time

Figure 4-7(a) The proposed AC stress degradation model in TFT structure with drain bias voltage when V_g swings from -15V to 0V with short rising time

Figure 4-7(b) The proposed AC stress degradation model in TFT structure with drain bias voltage when V_g swings from -15V to 0V with long rising time

Table 4-3 Setting of time for the experiment of T_f from 100ns to 700ns

Figure 4-8 The three stressed condition with T_f from 100ns to 700ns

Figure 4-9(a) Dependence of the mobility after gate AC stress in the off region on falling time

Figure 4-9(b) Dependence of the S.S. after gate AC stress in the off region on falling time

Figure 4-10 The pump current under various gate pulse falling time

Figure 4-11(a) The measured DC drain current versus stress time under gate pulses

with various falling time

Figure 4-11(b) The measured DC drain current versus stress time under gate pulses

with various falling time

Figure 4-12(a) The proposed AC stress degradation model in TFT structure with drain bias voltage when V_g swings from 0V to -15V with short falling time

Figure 4-12(b) The proposed AC stress degradation model in TFT structure with drain bias voltage when V_g swings from 0V to -15V with long falling time

Figure 4-13 TFT under various V_g range stress with drain bias

Figure 4-14(a) The mobility extract under various V_{DS} and V_g range

Figure 4-14(b) The sub-threshold swing extract under various V_{DS} and V_g range

Figure 4-15 Normalized (a)(c)(e)(g) C_{GS} (b)(d)(f)(h) C_{GD} curve (after AC stress with drain bias) versus drain voltage at frequencies 1M Hz

Figure 4-16 The electric field under various gate range AC stress with drain 20 V

Figure 4-17 The highest electric field under various V_g voltage

Figure 4-18 The pumped current measure under various gate pulse range

Figure 4-19 The measured DC drain current under various V_g range AC gate stress with drain 20 V